# Communications Research Centre

# A COHERENT LABORATORY RADAR SYSTEM

by

F.E. Smith



DEPARTMENT OF COMMUNICATIONS
MINISTÈRE DES COMMUNICATIONS

CRC TECHNICAL NOTE NO. 628



CANADA

OTTAWA, FEBRUARY 1970

COMMUNICATIONS RESEARCH CENTRE

DEPARTMENT OF COMMUNICATIONS
CANADA



# A COHERENT LABORATORY RADAR SYSTEM

by

F.E. Smith

*(National Communications Laboratory)*



**CRC TECHNICAL NOTE NO. 628**

*Published February 1970*

OTTAWA



70-059

TABLE OF CONTENTS

# A COHERENT LABORATORY RADAR SYSTEM

by

F.E. Smith

ABSTRACT

This technical note proposes a coherent laboratory radar system for conducting studies on digital MTI subsystems subjected to real clutter environments. Some fundamental design considerations for a coherent pulsed system are presented. In particular, the digital signal processing channel, the system dynamic range, the estimated clutter return levels and the influence of system errors on the clutter cancellation ratio are discussed. Several systems extensions to incorporate such techniques as frequency agility, coded waveform design, electronic antenna scanning and adaptive digital processing are introduced to indicate the growth potential of the proposed coherent laboratory system.

## 1. INTRODUCTION

For the past several years the Communications Research Centre (CRC), formerly the Defence Research Telecommunications Establishment (DRTE), has been investigating Air Traffic Control radar problems for the Canadian Armed Forces, both in Central Europe and in Canada[1,2].

Ground clutter and precipitation clutter, separately and in concert, contributed to some of the difficulties encountered. In these cases the MTI performance of the radars currently employed was found to be inadequate. Some of these problems, such as instabilities and unreliable operations over long time periods, were attributable to the MTI subsystems. Other MTI problems such as the limitations imposed by antenna scanning modulation and frequency modulation of the magnetron transmitters, were concerned with the radar system design as a whole.

In view of these problems, CRC undertook a research program aimed at improving the operational performance of MTI subsystems. Owing to the instability, unreliability and lack of flexibility encountered in existing analogue MTI systems, a decision was made to investigate digital MTI techniques. The technical requirements for the first digital system were influenced by the information obtained from the investigations mentioned above and will be considered later in this TN. It is emphasized that these considerations apply to the preliminary design and do not reflect the more demanding criteria envisaged for future research in this area.

A capability for testing realistically such a digital MTI system under actual clutter conditions did not exist within CRC. In addition, the specification for the technical parameters needed for futuristic MTI systems required much more information on clutter behaviour than that in existence at the time. Furthermore, a modern, flexible, low-power laboratory radar was needed to conduct research on adaptive radar techniques and, in particular, on adaptive digital filtering techniques. For these reasons, the CRC Radar Section undertook the development of a flexible, coherent, low-power radar system for laboratory use.

Some basic design considerations for this coherent laboratory radar are the subject of the TN. The initial system is being constructed, for the most part, with existing laboratory equipment and thus suffers certain constraints which are mentioned at appropriate places throughout the text.

## 2. REMARKS ON CLUTTER PROFILE STUDIES AND CLUTTER STATISTICS

Although not necessarily germane to future research investigations, it was considered that the information obtained from the ground clutter profiles studied earlier should be employed in the design of the digital MTI subsystem.

Clutter profiles obtained for a number of radars, in widely separated geographic locations, showed that most of the significant ground clutter was not more than 40 dB above the minimum detectable signal level (MDS) of the system. Peak clutter levels of 80 dB above the MDS level were observed at some sites; however, the occurrence of ground clutter in the 40-80 dB above MDS category was such that only a small fraction of the total display area--less than 14 per cent on a 15 nm range display for the worst case--was occupied by this strong clutter. In general then, a radar system of the type investigated would be satisfactory, for operations, if it possessed an actual MTI reference gain of 40 dB. Where the MTI reference gain is defined by:

$$G_0(v) = \frac{\text{MTI output signal-to-clutter power ratio}}{\text{MTI input signal-to-clutter power ratio}} .$$

The dynamic range of the digital MTI subsystem is conveniently indicated by the number of amplitude bits which are employed. Each bit doubles the number of voltage levels used to represent a continuous signal; hence, each bit adds six dB to the dynamic range. The coherent radar dynamic range requirement is a complicated function of the false alarms allowable, the clutter statistics

and other factors to be discussed in greater detail later in the paper. The dynamic range chosen for the initial digital filter was 54 dB corresponding to a nine-bit implementation. Usually, in a bipolar signal configuration, a nine-bit system yields 48 dB dynamic range because one bit is required for the determination of sign of the signal. However, an offset bias to the bipolar video will be used in the present system so that the full nine bits should contribute to the dynamic range.

Unfortunately, detailed clutter statistics were not obtained in the early investigations. The statement that all clutter processes are zero mean gaussian random processes is valid when the statistical evaluation includes all possible configurations of the scattering elements. For a fixed ground-based radar system, the environment consists of permanent scattering elements which are always present. This additional information can be most useful in the analysis of MTI systems. The constant component returned from these permanent scattering elements leads to non-zero average or mean values. If the random component is assumed to be gaussian, then the result is a non-zero mean, gaussian random process characterized by a magnitude that possesses a Rice distribution.

In any event, some statistical model of the clutter distribution is required for system analysis. A number of authors have indicated that many clutter environments of interest are generally described by the incoherent point scattering model[3,4,5]. Such evidence provides some justification for the use of a Rayleigh scattering model to represent the clutter scattering statistics. Analytical studies involving the 'one dominant' scattering model and generalized Rayleigh processes are available[6,7,8]. Although some experimental results have shown reasonable agreement with the Rayleigh scattering model, there is still need for detailed investigations of the region of the 'tail' of the statistical distributions. As the radar resolution cell size decreases the number of point scatterers may become small and it may not be reasonable to invoke the central limit theorem. Because these clutter distributions are of much concern to the MTI system designer, yet another reason emerges for building a coherent radar possessing the flexibility required for an investigation of such clutter characteristics.

It is necessary to assume some value for the average clutter radar cross-section per unit incidence area $\sigma^0$. The ground surface backscatter is a function of surface roughness, angle of incident energy, polarization, complex dielectric constant of the surface, and frequency. The available information on $\sigma^0$ at the frequency of interest here (S-band) is quite sparse[5,9,10,11,12]. The value of $\sigma^0$ chosen for these preliminary calculations was - 15 dB. The relation between $\sigma^0$ and $\sigma$, the total cross-section of all the individual scatterers located within the area of the antenna beam projected on the earth's surface, is

$$\sigma^0 = \frac{2\sigma}{\beta RCT \sec\theta} . \qquad \ldots\ldots (2.1)$$

The quantities used in this equation are defined in Appendix I.

# 3. GENERAL DESIGN CONSIDERATIONS

## 3.1 SIGNAL PROCESSING

### 3.1.1 General

The high reliability provided by integrated electronic circuitry makes feasible the incorporation of quite complicated digital signal processing techniques in the system design. In fact, a key point in the design of the laboratory radar is the digital instrumentation which should have the growth potential and flexibility to accommodate research studies encompassing a wide variety of interests. In particular, it is envisaged that the digital signal processing employed in the coherent radar system will evolve into a complex system for studying adaptive techniques.

Initially, however, the signal processing for this coherent pulsed system will be concerned with studies on clutter cancellation filters. The storage capacity to meet the filtering requirements is crucial in the signal processor design. Regardless of the technique employed, the filter parameters must be capable of large changes to accommodate the wide variety of conditions expected. The difficulty with analogue processors, such as delay lines and storage tubes, is that they exhibit problems with stability, maintenance and reliability and, in general, lack the flexibility for conducting experimental research on anti-clutter techniques.

An important parameter, in determining system performance in a coherent pulsed radar, is the clutter doppler bandwidth because a rejection filter must be placed about each multiple of the pulse recurrence frequency to eliminate the clutter. Wide clutter bandwidths reduce the clear region available for detecting desired targets between the rejection bands. Studies of clutter doppler bandwidths will be possible with the coherent laboratory system and should yield information required in the design of digital filters for optimizing the laboratory radar system performance. Studies concerned with adaptive techniques will also be possible.

Whereas in an operational system there is a prime requirement for avoiding 'blind speeds' in order to see targets possessing all velocities of interest, the laboratory system will not be concerned initially with this limitation. Because of the short unambiguous range of the system, a high pulse recurrence frequency (PRF) may be used. The power output of the coherent pulsed radar will be low so that even targets having large backscatter cross-sections will not be detectable beyond a few nautical miles. Thus, if the maximum unambiguous range is 10 nm, the PRF may be as high as 8.08 kHz. For operation at about 3 GHz, the corresponding blind speeds occur at

$$V_B \approx \frac{n(PRF)\lambda}{100} \approx \frac{n(PRF)}{10} \text{ knots}$$

$$= n\ (808) \text{ knots} \qquad \ldots\ldots\ (3.1)$$

where n is an integer, and $\lambda$ is the operating wavelength expressed in centimeters. The first blind speed occurs at 808 knots for such conditions.

Digital signal processing lends itself to great programming flexibility and, in particular, there is no rigid constraint on the radar interpulse period (determined by a fixed delay line length in the analogue system). Multiple PRF's may be employed; hence, there is great flexibility in the ability to shape the MTI response curves. Of course, the blind speed region in the vicinity of zero target doppler is inescapable because this is the region where the clutter exists. It is this region which requires detailed study. This study should be much easier to conduct on the laboratory system since many of the important parameters will be under rigid control. The clutter environment will be real; however, the target echo immersed in this clutter may be simulated by an RF signal generator, offset in doppler frequency in a controllable and known amount, by a serrodyne technique for example; and in addition, precision microwave attenuators may be used to control the return energy accurately.

### 3.1.2 Range-Gated Doppler Filter Techniques

Initially, the system is expected to be operated with the antenna rigidly fixed and there is to be no intentional antenna scanning modulation. A selected patch of clutter is to be illuminated and a large number of 'hits' will be a characteristic of the system. There is thus a distinct possibility of employing a range gated doppler filter signal processor with its inherent high degree of velocity resolution and concomitant high degree of clutter discrimination. The range gated doppler processor does not use delay line storage and, in this respect, possesses the advantage of allowing flexibility in the radar interpulse period. The equipment complexity would not impose any difficulty for the laboratory system since there would be few range bins involved in this short-range radar. For these reasons, the implementation of such signal processing will be considered during the early stages of development. However, the technique has limited practical applications because of the low number of successive target hits available in most mechanical scanning radars.

It should be mentioned that, in the long term, the coherent laboratory system may well employ an electronically scanned array. Such arrays allow increased system flexibility. For example, in heavy clutter areas the antenna beam may be brought to rest momentarily and the number of hits increased greatly to provide superior MTI processing. Under such conditions, the opportunity exists for great flexibility in terms of changing the false alarm rate, the data rate, and the detection mechanism and for the introduction of adaptive techniques.

### 3.1.3 Frequency Diversity and Integration Techniques

Integration techniques are well known for the enhancement of a desired signal in a thermal noise environment. Unfortunately, clutter processes differ markedly from thermal noise processes because a given clutter sample may remain correlated for a long time period. This correlation time is determined by the natural decay of a particular arrangement of clutter scatterers within the radar resolution cell. A number of radar systems perform a good deal of their integration within the clutter correlation time so that little target-to-clutter signal ratio enhancement is obtained. One way to circumvent this difficulty is to employ frequency agility. The amplitude and phase vector of the clutter in a given radar resolution cell is determined by the sum of the vector contributions of the returns from the individual scatterers within the cell. Because of the spacing between these scatterers, the phasing of these vectors

is determined by the radar operating frequency. A carrier frequency change results in a new amplitude and phase for the clutter return. If the frequency change for successive radar transmissions is large enough--of the order of the system bandwidth--the clutter amplitude and phase returns become independent. The compatibility of frequency agility processing with MTI processing is an area for study. Such studies should be helpful in determining optimum processing methods for operation in environments of combined ground clutter and rain clutter.

### 3.1.4 Coded Waveform Design

If the clutter is volume or area distributed, there is an advantage in reducing the size of the radar resolution cell to the physical size of the desired target. This may be achieved, in a number of instances, by signal coding techniques which should be considered for future application to the laboratory system.

### 3.1.5 The Signal Processing Channel

Initially, video filtering is proposed for the coherent pulse radar system. A single signal processing channel of this type cannot completely represent the signal and noise because such representation requires both in-phase and quadrature samples. A two-channel signal processing system provides N in-phase samples and N quadrature samples for N input pulses of signal and noise. In the two-channel configuration the in-phase and quadrature samples are independent and the system performance may be obtained by reference to the work of Marcum and Swerling[6]. In contradistinction, the single signal processing video channel provides N in-phase samples and no quadrature samples. As the samples are independent, there should be correspondence between this single-channel system and a two-channel system that has the equivalent of N/2 in-phase samples and N/2 quadrature samples. Thus, the single-channel system signal-to-noise performance should correspond to the performance, calculated by Marcum and Swerling, of a two-channel configuration where the effective number of integrated pulses is N/2.

The advantage of the two-channel signal processing configuration is that the sensitivity to target phasing effects is avoided, the signal-to-noise ratio required for a given probability of detection at a fixed false alarm rate is reduced, and the redundancy inherent in such a system increases the reliability.

The disadvantage of the two-channel processor is the increased complexity and cost.

Because the drawbacks of the single-channel video processor are not of prime significance in the foreseen initial use of the coherent laboratory radar, the single-channel configuration will be employed. The dwell times for the laboratory system can be extremely large compared to those attainable in a narrow beam scanning system; thus, N/2 can represent a large number of samples. It is also possible to have the target phase under the control of the laboratory system operator. Nonetheless, it is envisaged that, at a later date, a two-channel signal processor will be introduced into the system to investigate the practical difficulties of implementing such a processor.

## 3.2 SYSTEM DYNAMIC RANGE

Because the system dynamic range influences the actual clutter rejection achievable, it is a most important parameter.

The largest signal which the system must process is usually the clutter signal and, ideally, it must be handled without distortion. Clutter signals processed in a nonlinear channel introduce harmonics which fall outside the clutter filter rejection band and may generate system false alarms. Such false alarms may be prevented if the rms clutter value is held to a suitable level below the system saturation level. As mentioned in Section 2, typical clutter exhibits a Rayleigh amplitude distribution. Such a simple clutter model allows the calculation of the probability that a Rayleigh clutter distribution will exceed any given level. These calculations are carried out in Appendix II and presented graphically in Figure 2 (page 15).

The information from Figure 2 may be used to obtain the average time between saturation occurrences. This average time is helpful to the system designer and is obtained from the following relation

$$T_A = \frac{1}{\Delta f P_s} \quad , \qquad \ldots\ldots (3.2)$$

where $T_A$ = the average time between saturation occurrences,

$\Delta f$ = the clutter bandwidth,

$P_s$ = the probability of saturation.

Thus, if the system designer requires an average time between saturation occurrences of 3600 seconds on clutter whose bandwidth is 10 Hz, then

$$P_s = \frac{1}{\Delta f T_A} = 2.78 \times 10^{-5}$$

and from Figure 2 the ratio of the saturation level to rms level of the clutter must be set and held at 3.25.

The previous discussion refers to clutter possessing Rayleigh amplitude statistics. It is anticipated that a radar system such as the coherent laboratory radar will permit extension of these results by allowing the development of more realistic clutter models. In the early phases of the system operation, where a given clutter patch will be continuously illuminated, there should be no difficulty in adjusting the saturation-level-to-rms-clutter-level ratio. As the system is extended to the point where many range bins and azimuthal angles are employed, there will be a need for a false-alarm rate (CFAR) technique. Perhaps the simplest device to perform the CFAR task is the amplitude limiter. Nishikawa[16] has shown that such nonlinear MTI signal processing severely degrades the system performance when the clutter has a Rayleigh amplitude distribution. Nishikawa also has shown that, in such systems, the probability of detection may be increased considerably by the use of partial limiting as opposed to hard limiting. The performance of nonlinear MTI systems for more realistic clutter models is a subject for continuing research.

As explained in Section 2, the desired signal may be much smaller than the input clutter signal. The desired signal is competing, in general, with the quantization noise and must exceed it by an amount commensurate with Marcum's[6] curves to yield a desired detection probability. The rms quantization noise at the output of the A/D converter is $1/\sqrt{12}$ of one quantization level, corresponding to 10.8 dB below one quanta, for noise-like clutter signals[17].

Thus, a reasonable measure of the required system dynamic range is given by the ratio of the clutter input level to the rms quantization noise and this range may be expressed in dB as

$$\left[6\ (\text{total bits}) - \left\{\frac{\text{Saturation level}}{\text{rms clutter level}}\right\}_{dB} + 10.8\right] \text{ dB.}$$

This expression ignores the system thermal noise and thus, for a considerable range of practical operating conditions, it yields an approximate value for the system dynamic range.

A simple rule, often stated, for the dynamic range is six dB per amplitude bit. It is seen that this simple rule applies if the saturation-level-to-rms-clutter-level ratio is 10.8 dB, or 3.47. From Figure 2, it is seen that a saturation-to-rms-clutter-level ratio of 3.47 corresponds to a saturation probability of about $7 \times 10^{-6}$.

If, for example, the clutter bandwidth is 14.3 Hz, then equation (3.2) shows that the average time between saturation occurrences for a saturation probability of $7 \times 10^{-6}$ is $10^4$ sec. For system operation at a PRF of 3 kHz, the number of pulses transmitted during this interval would be $3 \times 10^7$. Hence, on the average there would be one sample point, out of every $3 \times 10^7$ available samples, in error because of the distortion introduced by the receiving system dynamic range constraint.

## 3.3 ANTENNA CONFIGURATION

A parabolic dish, possessing the following characteristics at S-band is available for use in the initial system configuration:

Antenna gain, G = 32 dB,

Polarization - horizontal,

Azimuthal beamwidth (3 dB points), $\beta$ = 2.0 degrees,

Near-in sidelobes 18 dB down,

Maximum cross polarization = - 25 dB.

The antenna mount is a rigid structure located 55 feet above ground level, and capable of locking the boresight axis on any desired azimuth over a vertical range of ± 15 degrees with respect to the horizontal.

A logical extension to the coherent laboratory radar system would be the addition of an electronically scanned array (Section 3.1.2).

## 3.4 FREQUENCY OF OPERATION

The most coherent microwave source available in the laboratory at present is an S-band signal source. Fortuitously, it is radar systems in this frequency band that have been under investigation. Future extensions of the coherent system will undoubtedly include other operating frequencies as and when the need arises.

## 3.5 RECEIVER NOISE FIGURE

The first breadboard version of the coherent system employs a tunnel diode amplifier stage. The noise performance of the receiver front end is degraded by feed line and circulator losses. The estimated noise figure for the receiving system is 7 dB: however, there should be no difficulty in reducing this figure by 3 to 4 dB in future versions of the system.

## 3.6 ESTIMATED CLUTTER RETURN LEVELS

A block diagram of an experimental breadboard version of the non-digital portion of the laboratory system is shown in Figure 3 (page 18).

The measured transmitter power at the antenna terminals is 200 milliwatts. It is now possible to calculate the expected clutter return levels based on the aforementioned clutter models and system parameters. These calculations are carried out in Appendix III.

As shown in Appendix III, it is concluded that the expected clutter return levels are satisfactory for conducting experiments on the first digital signal processor now being constructed. However, the more sophisticated digital signal processing subsystems planned for the future will place greater demands on the overall system performance. In particular, it is planned to investigate higher order MTI cancellation subsystems and the influence of system nonlinearities upon the cancellation ratios achieved.

## 3.7 TARGET IN CLUTTER RETURNS

Targets of opportunity are readily provided, in the vicinity of the laboratory site, by the vehicular traffic on nearby roadways and by rail traffic on an adjacent railway line. However, for precise measurements it is envisaged that special targets will be constructed whose effective backscattering cross-sectional area is well known and whose doppler return frequency is controllable.

## 3.8 SYSTEM ERRORS

The cancellation ratio, defined for fixed target returns as the ratio of the average power in the non-fluctuating portion of the radar return to the average power in the fluctuating portion of the return, is entirely dependent upon the coherent system errors attributable to equipment instabilities. It is necessary to perform an error analysis to determine what system instabilities are allowable if the clutter cancellation ratios desired are to be achieved.

Large cancellation ratios demand small system instability errors and it is anticipated that some of the measurement procedures necessary to isolate and to determine the various errors will require some thought and ingenuity.

Contributions to the instability noise are provided by pulse timing errors, pulse width errors, pulse amplitude errors, pulse distortions, phase and gain variations in the receiving networks, and phase and frequency errors in the transmitter and reference oscillators.

The system errors, at least for the initial experimental operation envisaged, are amenable to the statistical analysis introduced by Emerson[18]. The pertinent factors required for the present paper are presented in Appendix IV.

### 3.9 SYSTEM OUTPUT

Commensurate with the flexibility envisaged for the coherent laboratory system it is expected that, in addition to A-scan recording, chart recording and video tape recording techniques, a digital computer will be interfaced with the system. The digital computer will perform direct analysis, provide information to the automatic plotters for visual readouts and, eventually, provide the means for adaptive systems operation.

## 4. CONCLUSIONS

Experimental investigations conducted over the past several years at a number of radar sites have shown the need for improved MTI system performance. The advent of recent improvements in digital signal and data processing techniques has opened the way for the design and construction of a flexible coherent pulsed radar system. A number of fundamental design considerations for a laboratory system have been discussed and it is concluded that a low-power coherent system, suitable for carrying out studies on actual clutter processes and on improved digital MTI processing techniques, is feasible. Several systems extensions to incorporate such techniques as frequency agility, coded waveform design, electronic antenna scanning and adaptive digital processing, have been mentioned to indicate the growth potential of the proposed coherent laboratory system.

## 5. ACKNOWLEDGEMENTS

It is a pleasure to thank Mr. F.R. Cross of the CRC Radar Section for providing Figure 3 and several measured values used in the calculations.

## 6. REFERENCES


1. Smith, F.E., and F.R. Cross. January, 1969. Private communication.

2. Smith, F.E., and F.R. Cross. December, 1967. Private communication.

3. Kerr, D.E. (ed.) *Propagation of short-radio waves.* MIT Radiation Laboratories Series, Vol. 13, McGraw-Hill Book Co. Inc., New York, 1951.

4. Lawson, J.L., and G.E. Uhlenbeck. *Threshold signals.* MIT Radiation Laboratories Series, Vol. 24, McGraw-Hill Book Co. Inc., New York, 1950.

5. Skolnik, M.I. *Introduction to radar systems.* McGraw-Hill Book Co., New York, 1962.

6. Marcum, J.I., and P. Swerling. *Studies of target detection by pulsed radar.* IRE Trans. on Information Theory, Vol. IT-6, Special Monograph Issue, April, 1960.

7. Miller, K.S., et al. *Generalized Rayleigh processes.* Quarterly of Applied Mathematics, Vol. 16, No. 2, 1958.

8. Arens, R. *Complex processes for envelopes of normal noise.* IEEE Trans. on Information Theory, Vol. IT-3, No. 3, September 1957.

9. Li-Jen Du. *Rayleigh scattering from leaves.* Electro Science Laboratory Scientific Report No. 1, 21 January 1969.

10. Gent, H., et al. *Polarization of radar echoes, including aircraft, precipitation and terrain.* Proc. IEE, Vol. 110, No. 12, 1963.

11. McFee, R., and T.M. Maher. *Effect of surface reflections on rain cancellation of circularly polarized radars.* IRE Trans. on Antennas and Propagation, April, 1959.

12. Guinard, N.W., et al. *NRL terrain clutter study phase I.* Naval Research Laboratory, Washington, D.C., 10 May 1967.

13. Taylor, R.C. *Terrain return measurements at x, ku, and ka band.* IRE National Convention Record, Vol. 7, Part 1, pp 19-26, 1959.

14. Peake, W.H. *Theory of radar return from terrain.* IRE National Convention Record, Vol. 7, Part 1, pp 27-41, 1959.

15. Katz, I, and L.M. Spetner. *Polarization and depression angle dependence of radar terrain return.* National Bureau of Standards (US) J. Research, Vol. 64D, pp 483-486, September-October 1960.

16. Nishikawa, S. *Nonlinear processing of radar returns in MTI systems.* The Rand Corporation, RM-5490-PR, March 1968.

17. Bennett, W.R. *Spectra of quantized signals.* Bell Systems Technical Jour., July 1948.

18. Emerson, R.C. March 1954. Private communication.

# APPENDIX I

## RADAR TERRAIN RETURN

The geometry applicable to the coherent laboratory radar is illustrated in Figure 1. The illuminated area, A, is seen to be

$$A = \beta R \frac{CT}{2} \sec \theta_g \qquad .....(1)$$

where $\beta$ is the 3 dB azimuthal beamwidth of the antenna,

$R$ is the range to the centre of the illuminated clutter patch,

$C$ is the velocity of propagation of light,

$T$ is the pulse width,

$\theta_g$ is the grazing angle and for small ranges, such as those experienced for the proposed laboratory radar, the curvature of the earth may be neglected and the grazing angle is equal to the depression angle, $\theta$.

The illuminated area, A, is thus

$$A = \frac{\beta RCT}{2} \sec \theta. \qquad .....(2)$$

The average radar cross-section per unit illuminated area is hence

$$\sigma^0 = \frac{\sigma}{A} = \frac{\sigma}{\frac{\beta RCT}{2} \sec \theta} \qquad .....(3)$$

or

$$\sigma = \frac{\sigma^0 \beta RCT}{2} \sec \theta. \qquad .....(4)$$

It is envisaged that the pulse width, T, of the coherent pulse radar will be variable over a wide range of values; however, for convenience here, calculations are based upon a representative value for T of two microseconds.

The antenna to be used in the system is available in the laboratory and possesses a three dB beamwidth of 2.0 degrees or 0.035 rad.

For the assumed value of $\sigma^0 = -15$ dB, equation (4) reduces to

$$\sigma = 0.33\ R \sec \theta \qquad .....(5)$$

where R is the range in metres,

$\theta$ is the depression angle in degrees,

and $\sigma$ is the total backscattering cross-section in square metres.

The antenna height is 55 feet or 16.7 metres; hence, it is now possible to calculate values of R and $\theta$ for an assumed flat earth model. The variation in $\sigma$, corresponding to a variation in range of $R_1 = 304$ m to $R_2 = 3040$ m, is

$$\sigma_1 \approx (0.33)\ (304) \approx 100\ m^2,$$

to

$$\sigma_2 \approx (0.33)\ (3040) \approx 1000\ m^2.$$

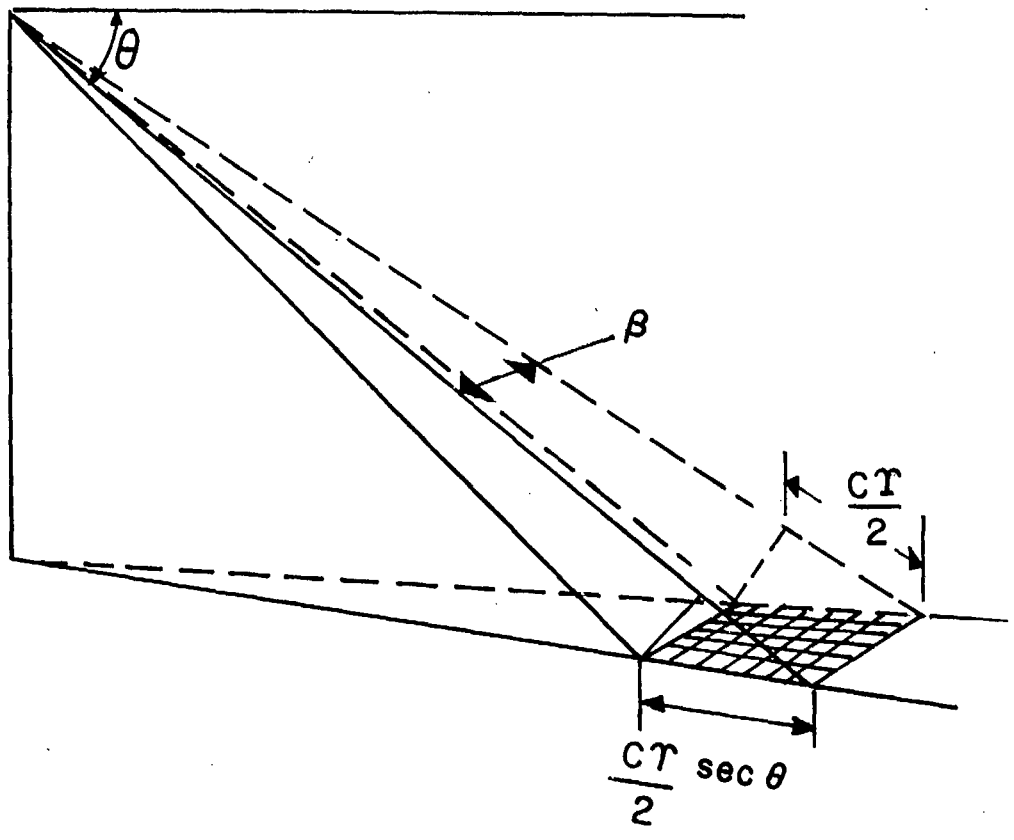


*Fig. 1. Radar terrain return geometry.*

# APPENDIX II

## CALCULATIONS OF THE PROBABILITY OF SATURATION BASED ON A RAYLEIGH CLUTTER MODEL

The probability density function for the Rayleigh clutter model in terms of the signal envelope (voltage) is given by

$$p(x) = \frac{2x}{\sigma^2} \exp\left(-\frac{x^2}{\sigma^2}\right), \quad x > 0 \qquad \ldots\ldots(1)$$

where $\sigma$ = the rms clutter level.

The probability that the clutter exceeds the level, $\psi$, is thus given by

$$\int_{\psi}^{\infty} p(x)\, dx = \int_{\psi}^{\infty} \frac{2x}{\sigma^2} \exp\left(-\frac{x^2}{\sigma^2}\right) dx$$

$$= -\int_{\psi}^{\infty} d\left[\exp\left(-\frac{x^2}{\sigma^2}\right)\right]$$

$$= -\left[\exp\left(-\frac{x^2}{\sigma^2}\right)\Big|_{\psi}^{\infty}\right]$$

$$= \exp\left(-\frac{\psi^2}{\sigma^2}\right).$$

Hence, if the saturation level, $\psi$, is three times the rms clutter level; i.e.,

$$\psi = 3\sigma \quad \text{or} \quad \psi^2 = 9\sigma^2$$

the probability of saturation is

$$\exp(-9) = 1.23 \times 10^{-4}.$$

A plot of the probability of saturation vs the ratio, saturation-level-to-rms-clutter-level, is given in Figure 2.

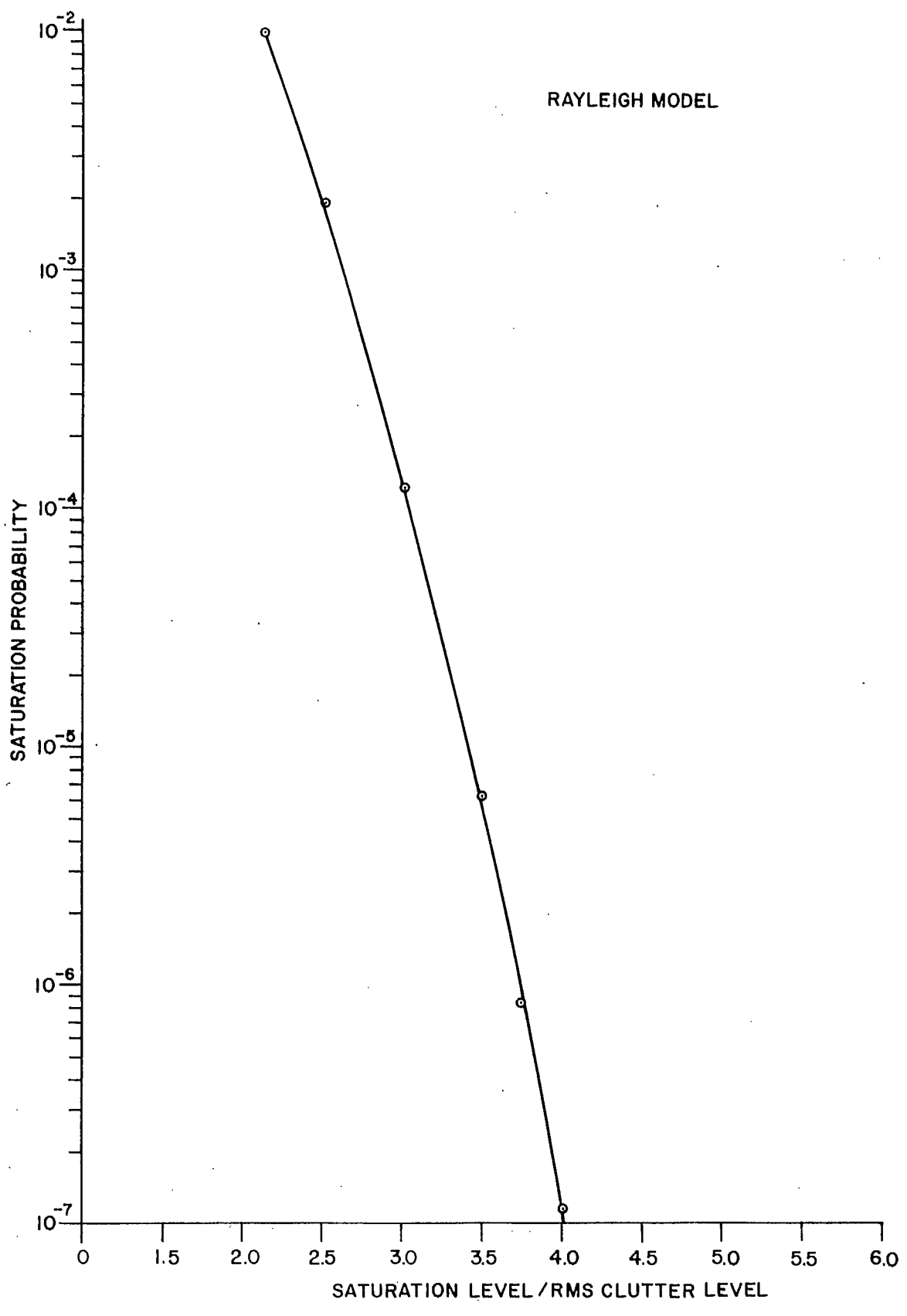


*Fig. 2. Saturation probability vs saturation level/rms clutter level.*

# APPENDIX III

## ESTIMATED CLUTTER RETURN LEVELS

From the radar equation,

$$P_{R1} = \frac{P_T G^2 \lambda^2 \sigma_1}{(4\pi)^3 R_1^4}$$

where $P_{R1}$ is the expected average clutter power received,

$G$ is the antenna gain,

$\lambda$ is the operating wavelength,

$\sigma_1$ is the backscattering cross-section of the clutter at the range, $R_1$, as calculated in Appendix I.

$R_1 = 304$ m

and $R_2 = 3040$ m.

Thus

$$P_{R1} = \frac{(200 \times 10^{-3})(1585)^2(0.1)^2(10)^2}{(1.98 \times 10^3)(3.04)^4(10)^8}$$

$$= 2.98 \times 10^{-8} \text{ watts},$$

The numerical values used have been discussed in the appropriate sections throughout the text.

Now the MDS level of the radar system is calculated from

$$\overline{NF}kTB$$

where $\overline{NF}$ is the receiver noise figure,

$k$ is the Boltzmann's constant

$T$ is the standard reference temperature

and $B$ is the receiver bandwidth.

As explained in Appendix I, the pulse width and hence the receiver bandwidth will be variable. For consistency, in the present calculation, the two microsecond pulse width used in deriving $\sigma_1$ is assumed. The value of the noise figure used is that given in Section 3.5. The resulting MDS level for the system is

$$\overline{NF}kTB = (5)(1.38 \times 10^{-23})(290)(0.5 \times 10^6)$$
$$= 1 \times 10^{-14} \text{ watts}.$$

Thus, the ratio of the expected average clutter return power level to the MDS power level is

$$\frac{P_{R1}}{P_{MDS}} = \frac{2.98 \times 10^{-8}}{1 \times 10^{-14}} = 2.98 \times 10^{6}$$

or approximately 65 dB.

$$\frac{P_{R2}}{P_{MDS}} = \frac{P_T G^2 \lambda^2 \sigma^2}{P_{MDS} (4\pi)^3 R_2^4} = 2.98 \times 10^{3}$$

or approximately 35 dB.

The conclusion is that the expected clutter levels are in a useful region for conducting experiments on the initial digital signal processor currently being constructed.

It should be noted that $P_T$ may be increased by several dB over the value obtained on the current breadboard system (Fig. 3) because there are excessive losses in the feedline and microwave components. Similarly, there is room for improvement of several dB in the receiver noise figure performance.

In addition, there are large stationary man-made reflecting surfaces in the vicinity of the laboratory, such as buildings, antennas and water towers. These structures should provide large stationary clutter returns that are useful for system clutter cancellation measurements.

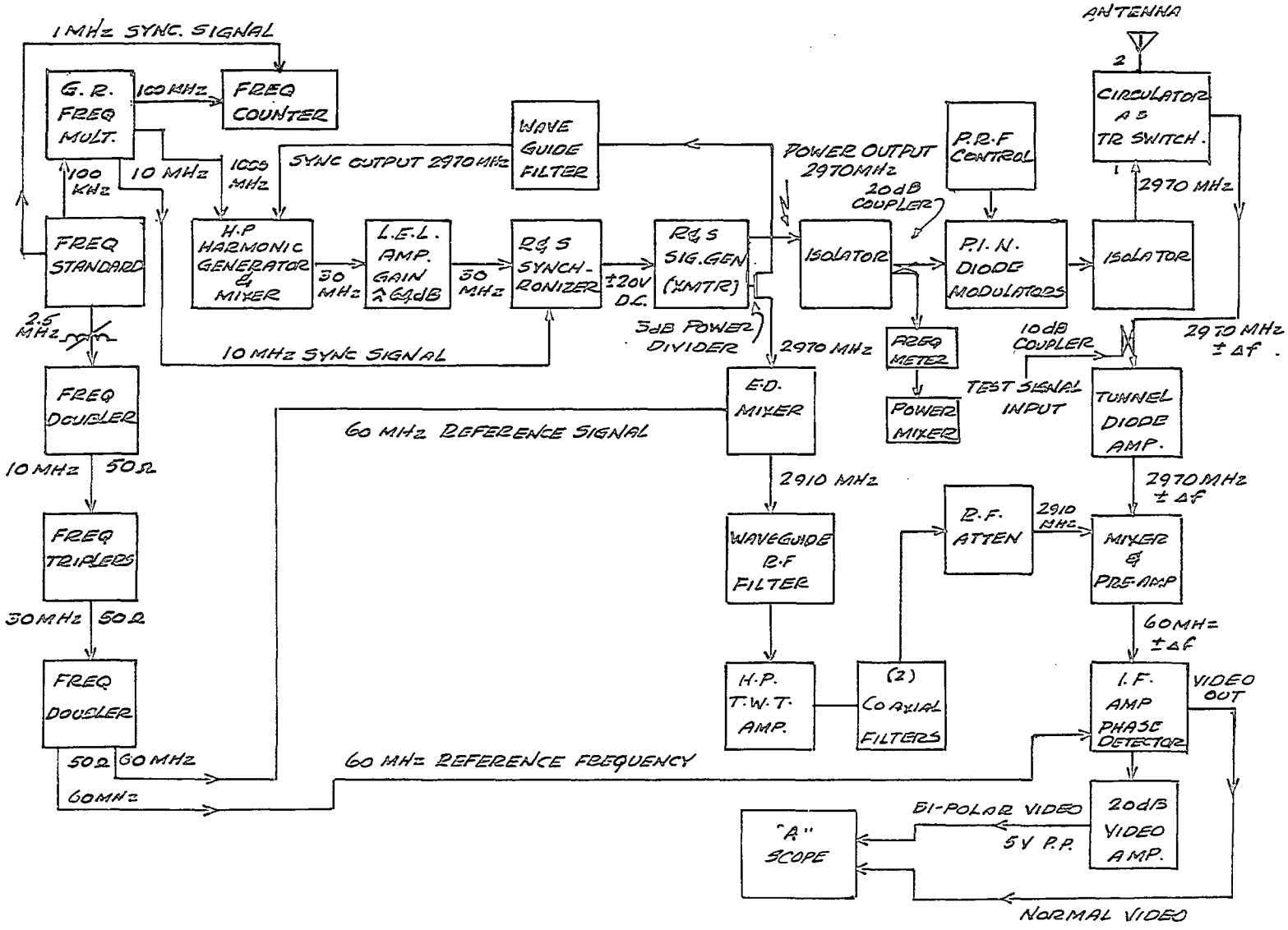


*Fig. 3. Experimental breadboard model.*

# APPENDIX IV

## SYSTEM ERRORS

Initially, the coherent pulse system will be operated as explained in Section 3.1.2. Under such circumstances it is permissible to regard the fixed target signal return, s(t), as a deterministic infinite train of pulses. The instability noise, n(t), is characterized by a random variable, independent from pulse to pulse, and distributed according to a normal law. The received signal function is thus the sum of the fixed target return voltage and the error noise voltage; i.e.,

$$s(t) + n(t).$$

The infinite pulse train, s(t) + n(t), may be rewritten as

$$s(t) + n(t) = \Big\{ s(t) + E\big[n(t)\big] \Big\} + \Big\{ n(t) - E\big[n(t)\big] \Big\} \qquad .....(1)$$

where $E\big[n(t)\big]$ is the mathematical expectation of n(t).

The non-fluctuating portion of the received signal function is thus

$$E\big[s(t) + n(t)\big] = s(t) + E\big[n(t)\big], \qquad .....(2)$$

and the fluctuating portion is

$$n(t) - E\big[n(t)\big]. \qquad .....(3)$$

The corresponding average powers for the non-fluctuating and fluctuating parts of the received signal function are thus

$$E\Big(\big\{s(t) + E\big[n(t)\big]\big\}^2\Big), \qquad .....(4)$$

and

$$E\Big(\big\{n(t) - E\big[n(t)\big]\big\}^2\Big), \qquad .....(5)$$

respectively.

Hence, the mathematical expression for the cancellation ratio, as defined in Section 3.8, is given by

$$C = \frac{E\Big(\big\{s(t) + E\big[n(t)\big]\big\}^2\Big)}{E\Big(\big\{n(t) - E\big[n(t)\big]\big\}^2\Big)}. \qquad .....(6)$$

For mathematical convenience, the signal pulses are assumed to have gaussian envelopes so that the $k^{\underline{th}}$ voltage pulse received may be written as

$$S_k(t) = \alpha \exp\left[-\frac{(t-t_k)^2}{2\beta^2}\right] \qquad .....(7)$$

where $\alpha$ = the peak pulse amplitude,

$t_k$ = the pulse epoch,

and $\beta$ = the pulse width.

As mentioned previously, the statistical parameters $\alpha$, $t_k$, and $\beta$ are assumed to have normal distributions.

Thus, if the random error in pulse timing is $\gamma$, the probability density function for $\gamma$ is gaussian with mean zero and variance $\overline{\gamma^2}$, or mathematically

$$P(\gamma) = \frac{1}{\sqrt{2\pi\overline{\gamma^2}}} \exp\left[-\frac{\gamma^2}{2\overline{\gamma^2}}\right]. \qquad .....(8)$$

In general, the instability noise is equal to the actual pulse received less the unperturbed signal pulse. For the particular instance where the only perturbation in the pulse received is attributable to a timing error, the noise voltage is given by

$$n(t) = \alpha \left\{ \exp\left[-\frac{(t-t_k-\gamma)^2}{2\beta^2}\right] - \exp\left[-\frac{(t-t_k)^2}{2\beta^2}\right]\right\}. \qquad .....(9)$$

Similarly, expressions for n(t) may be derived for the cases where the only perturbations are caused by amplitude errors alone or pulse width errors alone. By similar reasoning, expressions for n(t) may be derived for phase errors that arise in reference oscillators, the locking circuitry or through frequency modulation within the transmitted pulse.

The MTI gain, $G_0(v)$, is defined as[18]

$$G_0(v) = \overline{G_0}\, E(v) = \frac{(S/C)out}{(S/C)in},$$

where $\overline{G_0}$ = the MTI reference gain--dependent on the clutter characteristics but independent of target velocity,

$E(v)$ = the velocity enhancement function--independent of the clutter characteristics,

$(S/C)out$ = the output signal-to-clutter power ratio,

and $(S/C)in$ = the input signal-to-clutter power ratio.

For large cancellation ratios, such as required in modern MTI systems, the actual MTI reference gain, $\overline{G_a}$, may be expressed as

$$\overline{G_a} = \frac{1}{\frac{1}{\overline{G_0}} + \frac{1}{C}},$$

where C is the overall system cancellation ratio.

It is seen from this expression that the achieved MTI reference gain equals the ideal reference gain, $\overline{G_0}$, as the cancellation ratio approaches infinity.

For practical systems, the actual MTI reference gain will be less than $\overline{G_0}$ as determined by the value of the cancellation ratio. If $\overline{G_0}$ is required to be 40 dB (cf Section 2) both $\overline{G_0}$, which depends on the clutter characteristics and the MTI canceller performance, and the cancellation ratio must be greater than 40 dB.

The results of the calculations for the cancellation ratios, as determined by equation (6), are given below.'

The cancellation ratio obtained by assuming that errors are caused by amplitude perturbations alone, is

$$C_A = \frac{\alpha^2}{\overline{\Gamma^2}} \qquad .....(10)$$

where $\alpha$ is the unperburbed pulse amplitude, and $\overline{\Gamma^2}$ is the variance of the amplitude error distribution. This behaviour is shown graphically in Figure 4.

The cancellation ratio, obtained by assuming that errors are the result of pulse width perturbations alone, is

$$C_W = \frac{4}{3}\frac{\beta^2}{\overline{\psi^2}} \qquad .....(11)$$

where $\beta$ is the unperturbed pulse width, and $\overline{\psi^2}$ is the variance of the pulse width error distribution. This behaviour is illustrated in Figure 5.

The cancellation ratio, obtained by assuming that errors are the result of pulse timing perburbations alone, is

$$C_T = \frac{1}{\left(\sqrt{1 + \frac{\overline{\gamma^2}}{\beta^2}} - 1\right)} \qquad .....(12)$$

where $\beta$ is the pulse width, and $\overline{\gamma^2}$ is the variance of the pulse timing error distribution. This behaviour is shown in Figure 6.

The cancellation ratio, obtained by assuming that errors are the result of phase perturbations alone, is

$$C_\phi = \frac{1}{\cosh \overline{\phi^2} - 1} \qquad .....(13)$$

where $\overline{\phi^2}$ is the variance of the phase error distribution. The behaviour is shown in Figure 7.

For systems analysis it is necessary to find the overall system cancellation ratio by use of the individual cancellation ratios obtained in the foregoing. The effects of pulse distortion and phase and gain variations in the receiving networks are a matter of detail for the particular engineering implementation employed and will not be considered further here.

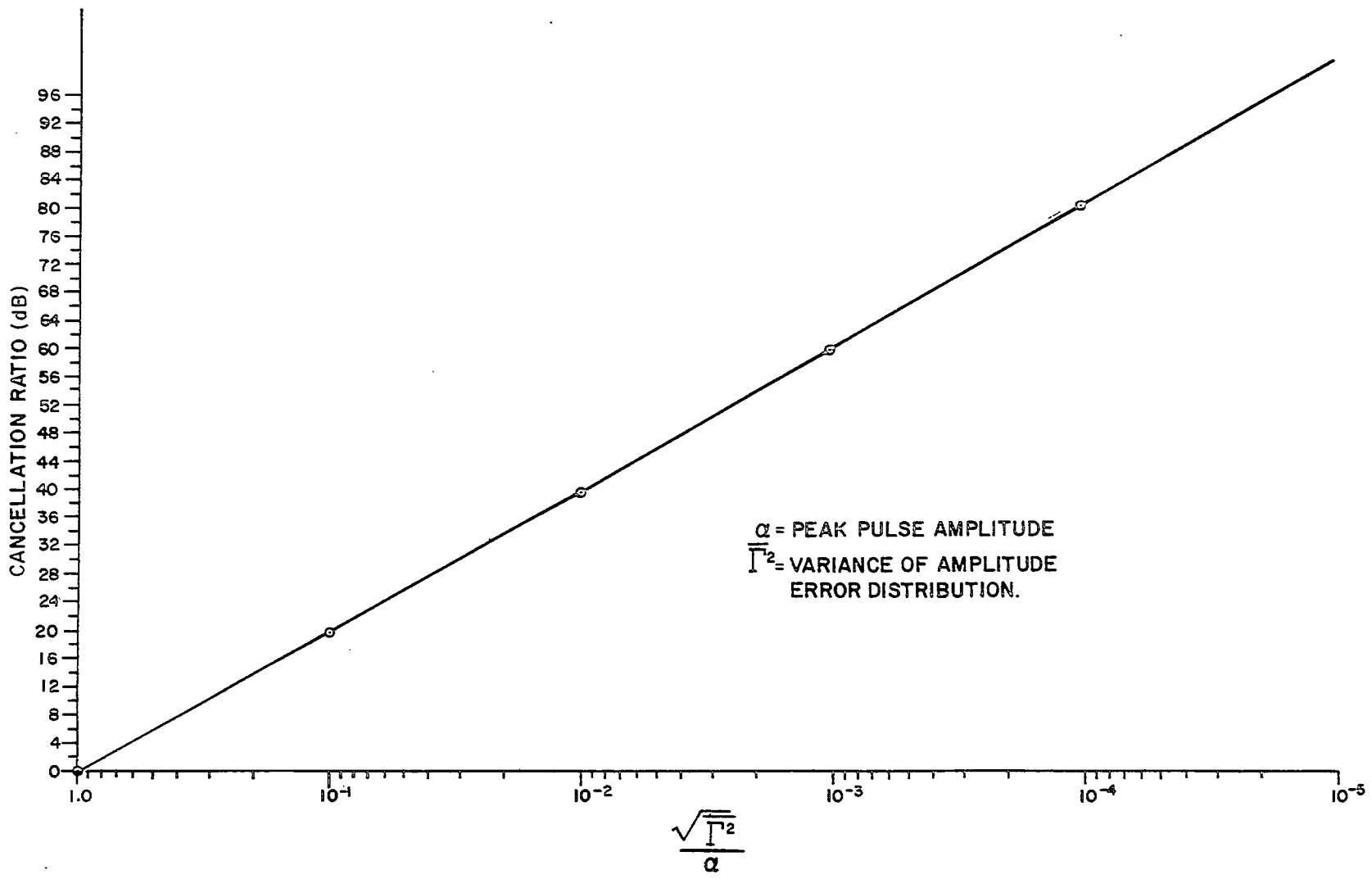


*Fig. 4. Clutter cancellation ratio for pulse amplitude error case.*

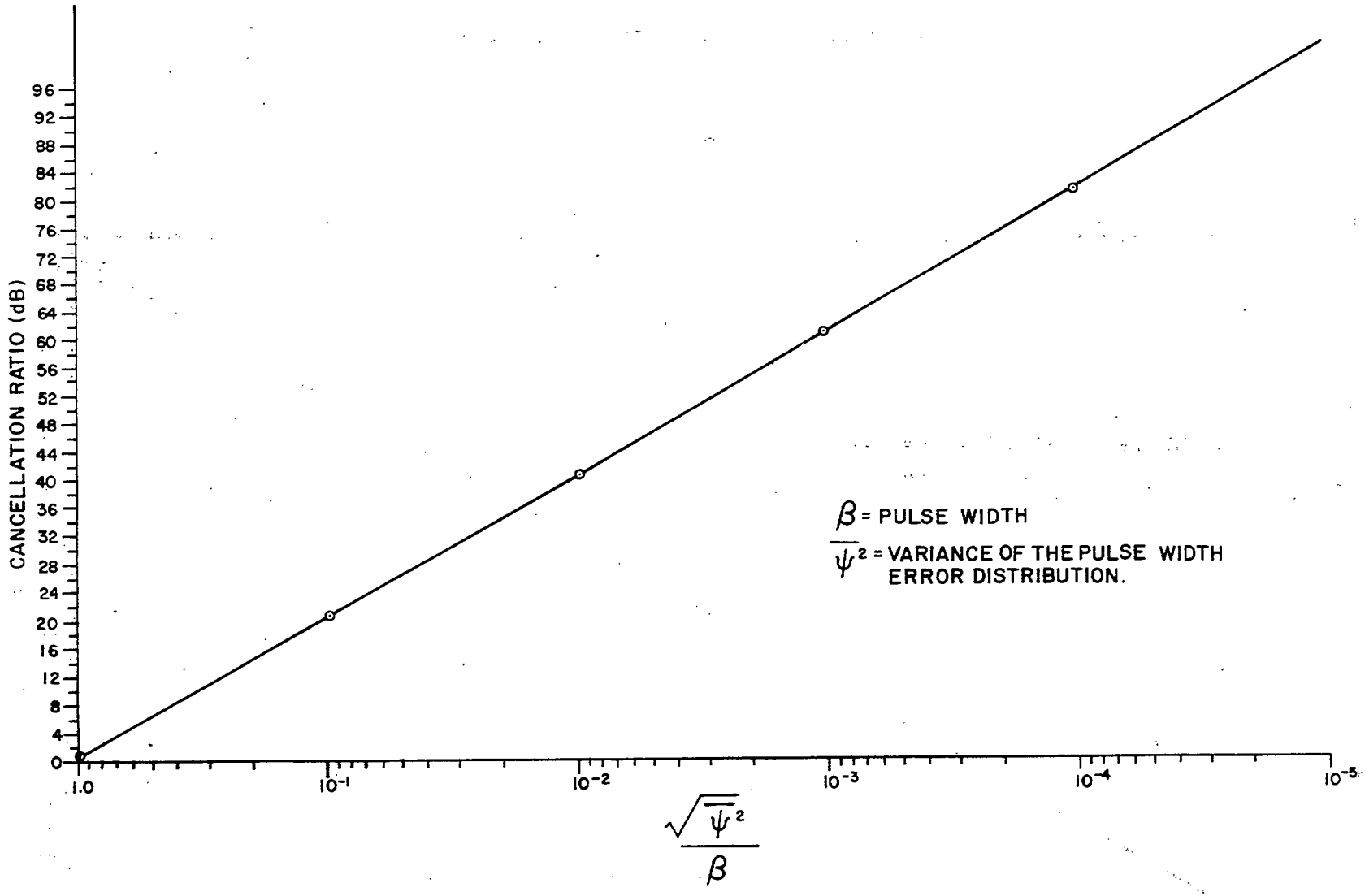


*Fig. 5. Cancellation ratio for pulse width error case.*

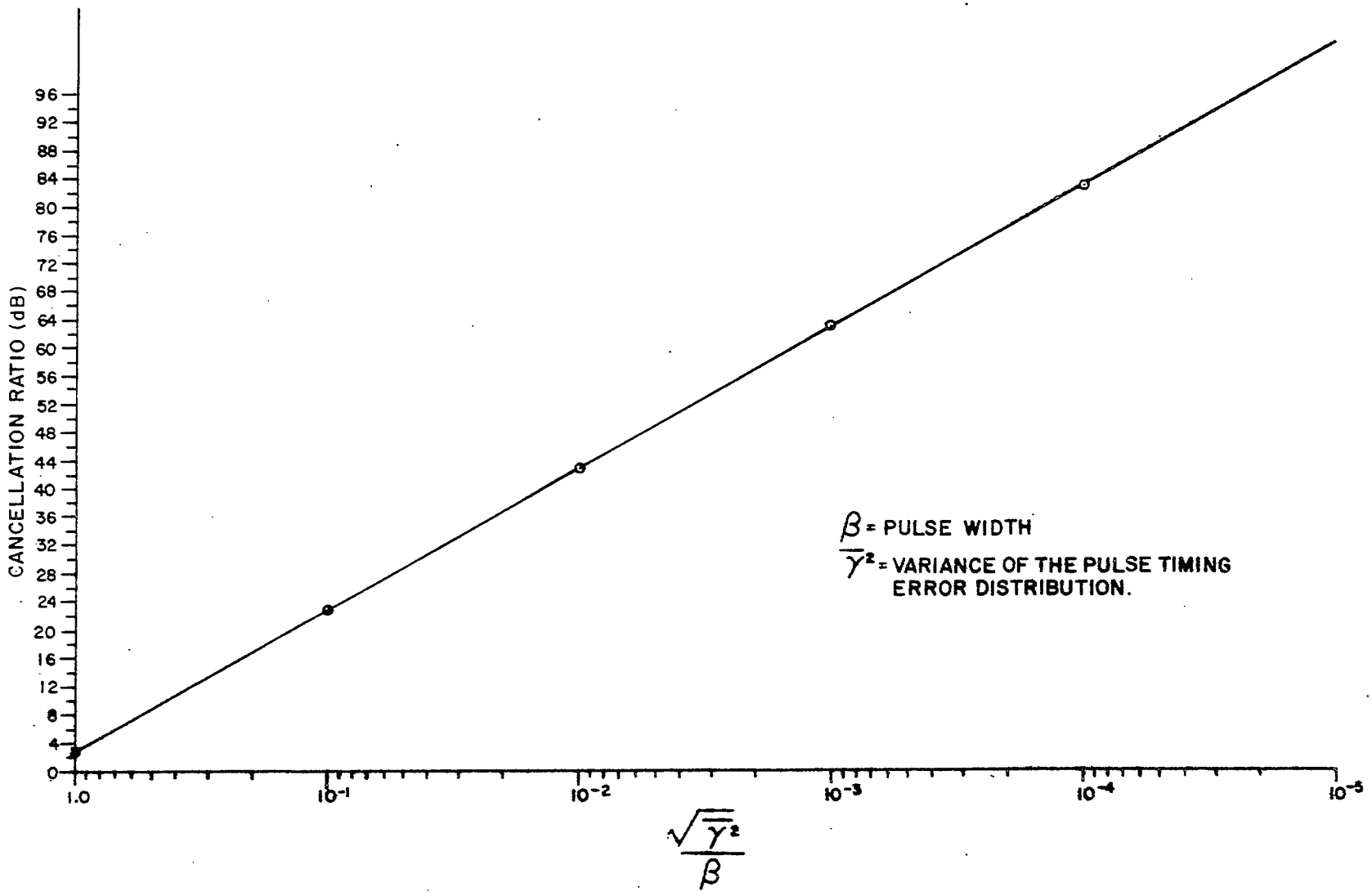


*Fig. 6. Cancellation ratio for pulse timing error case.*

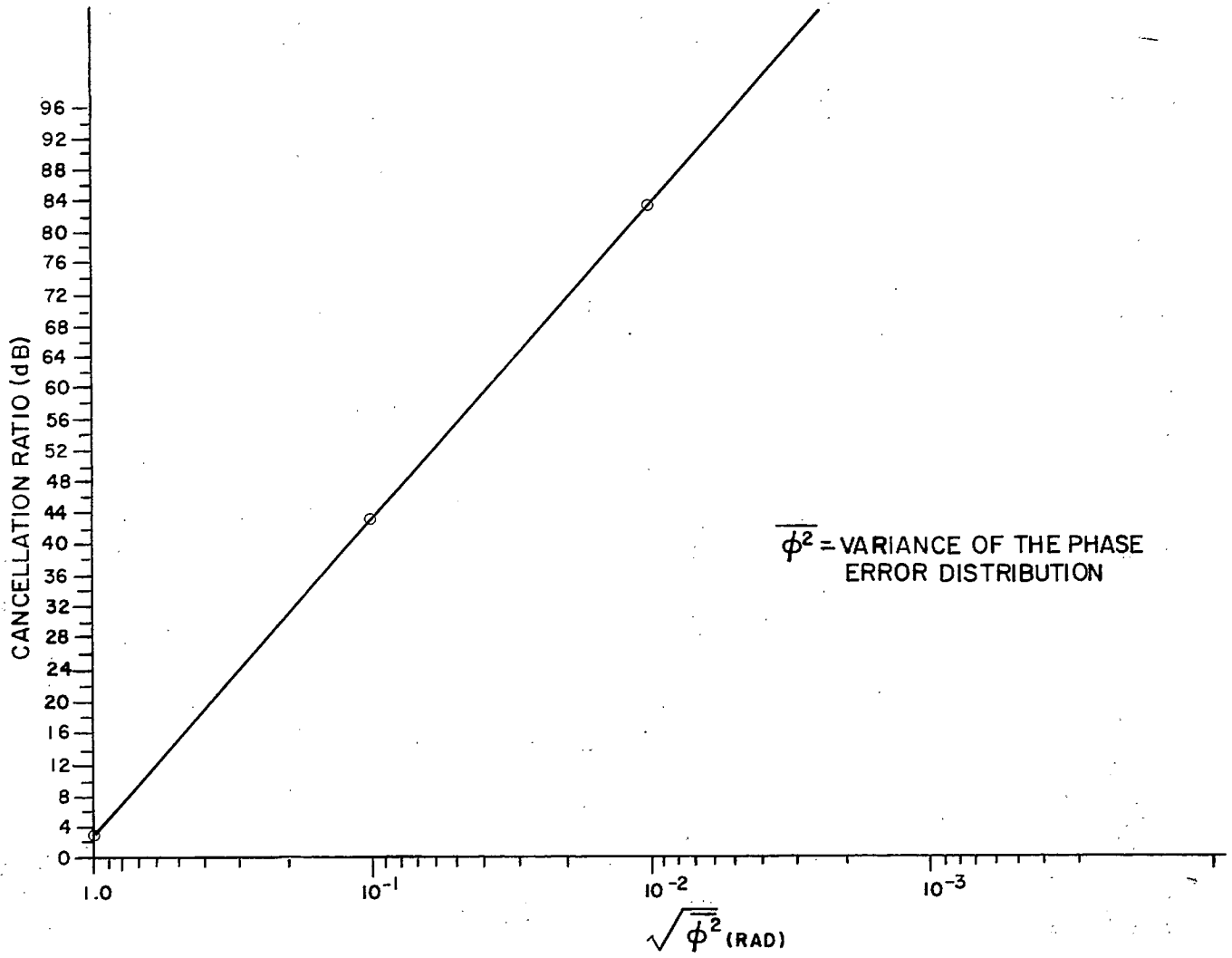


*Fig. 7. Cancellation ratio for phase error case.*

It is reasonable to assume that the contributing system errors are independent. The power of the fluctuating portions of the instability noises are additive under this assumption and the overall system cancellation ratio becomes

$$C = \frac{1}{\frac{1}{C_A} + \frac{1}{C_T} + \frac{1}{C_W} + \frac{1}{C_{\phi_1}} + \frac{1}{C_{\phi_2}} + \ldots} \qquad \ldots\ldots(14)$$

A sense of the quantitative values of the parameters involved is obtained by considering the following simple example. Assume that the error sources are all independent, the individual cancellation ratios are equal, there are two sources of phase error and the overall cancellation ratio required is 46 dB. Then equation (14) becomes

$$C = \frac{1}{5\,\frac{1}{C_{ind}}} = 40{,}000,$$

$$\text{or} \quad C_{ind} = 200{,}000, \text{ or } 53 \text{ dB}.$$

From Figure 4, it is seen that such a cancellation ratio corresponds to

$$\frac{\sqrt{\overline{\Gamma^2}}}{\alpha} = 2.3 \times 10^{-3}.$$

Thus for a peak amplitude equal to unity,

$$\sqrt{\overline{\Gamma^2}} = 2.3 \times 10^{-3}$$

corresponding to an rms amplitude error of 0.23 per cent.

From Figure 5, a 53 dB cancellation ratio corresponds to

$$\frac{\sqrt{\overline{\psi^2}}}{\beta} = 2.6 \times 10^{-3}.$$

Thus for a pulse width of $2 \times 10^{-6}$ sec

$$\sqrt{\overline{\psi^2}} = 5.2 \times 10^{-9} \text{ sec}$$

corresponding to a standard deviation in pulse width error of $5.2 \times 10^{-9}$ sec.

From Figure 6, a 53 dB cancellation

$$\frac{\sqrt{\overline{\gamma^2}}}{\beta} = 3.2 \times 10^{-3}$$

and for a pulse width of $2 \times 10^{-6}$ sec,

$$\sqrt{\overline{\gamma^2}} = 6.4 \times 10^{-9} \text{ sec},$$

corresponding to a standard deviation in pulse timing error of $6.4 \times 10^{-9}$ sec.

From Figure 7, a 53 dB cancellation ratio corresponds to

$$\sqrt{\overline{\phi^2}} = 5.6 \times 10^{-2} = 0.056 \text{ rad.}$$

corresponding to a standard deviation in phase error of 0.056 rad.

For a number of possible systems configurations involving two-pulse cancellers the influence of frequency errors has been treated in Skolnik[5].